1D MODELLING OF SOME PARADIGMATIC NON-IDEAL COMPRESSIBLE FLOWS

Francesco Tosto[1*], Claudio Lettieri[1], Matteo Pini[1], Piero Colonna[1]

[1] Propulsion and Power, Delft University of Technology,
Kluyverweg 1, 2629 HS Delft
f.tosto@tudelft.nl

* Corresponding Author

ABSTRACT

Systems based on the organic Rankine cycle (ORC) concept for energy harvesting, refrigeration and power generation make use of a variety of working fluids. For instance, complex working fluids and supercritical carbon dioxide are utilized in organic Rankine cycle and supercritical CO_2 Brayton cycle power systems. Thermo-fluid characteristics of these vapor flows in expanders or compressors deviate significantly from those of flows of perfect gases and this deviation increases if the processes occur in proximity of saturation or the vapor-liquid critical point. The term Non-Ideal Compressible Fluid Dynamics (NICFD) is utilized to characterize the gas dynamics of dense vapors: a key parameter to study these flows is the fundamental derivative of gasdynamics Γ, which accounts for variations in speed of sound with density over isentropic processes. Although rather extensive theoretical knowledge has been developed on the fundamental aspects of NICFD, these findings have not been thoroughly studied in the context of applications and particularly of energy conversion applications, i.e., flows in turbomachinery and heat exchangers. This study is aimed at evaluating the impact of NICFD effects by analyzing simple 1D flow configurations reproducing some of the main entropy loss mechanisms of turbomachinery. A new general theoretical framework based on quasi one-dimensional control volume analysis is developed: a new matrix of influence coefficients accounting for shaft work, heat addition, wall friction, variation in cross section area and mass injection in the control volume is derived. The approach is based on works by Shapiro (1953). Experimental observations of the expansion of a siloxane vapor in a de Laval nozzle provide a mean for preliminary validation. Simple Rayleigh and Fanno flow configuration are studied to quantify the impact of these phenomena on the performance of turbomachinery (and heat exchangers).

1. INTRODUCTION

Systems for power generation, waste heat recovery, refrigeration, oil and gas, chemical process industry and air liquefaction involve flows of dense organic vapours and supercritical fluids. For instance, organic substances such as siloxanes operate as working fluid for organic Rankine cycle (ORC) power systems (Colonna et al., 2015). The thermodynamic properties of these working fluids largely depart from those calculated under the ideal gas assumption. Several theoretical studies within non-ideal compressible fluid dynamics (NICFD) investigated the impact of the fluid non ideality on the gas dynamics (Thompson, 1971). In engineering, NICFD makes the design phases of system components more challenging. Standard design guidelines for conventional applications cannot be employed as their use would lead to wrong performance predictions.

The design of turbomachinery for NICFD application is mainly based on empirical correlations. Studies in the literature report innovative methodologies for preliminary fluid dynamic design (Bahamonde et al., 2017) and optimization (Rosset et al., 2018) of turbines for ORC power systems, but no general guidelines for NICFD turbomachinery are available yet. De Servi et al. (2019) utilized conventional statistical diagrams and the methodology by Bahamonde et al. (2017) for the meanline design of a radial inflow turbine for a mini ORC power system operating with siloxane MM. The difference between the

efficiency calculated after a CFD shape optimization and the efficiency estimated by the preliminary design is ~ 1.6%. Improved guidelines for preliminary meanline design would thus provide more accurate predictions of both performance and loss breakdown of turbines and compressors operating in NICFD. Denton (1993) proposed for the first time a general loss model for turbomachinery purely based on physics. His results, however, are valid only under both the ideal gas and the incompressible flow assumptions.

This paper focuses on the theoretical analysis of simple one dimensional NICFD flow configurations. A general one dimensional theoretical framework for NICFD is introduced (section 2). Simple relations based on one-dimensional conservation equations are derived for non ideal compressible flows by following the same approach utilized by Shapiro (1953) for ideal gases. The derived framework can be used for preliminary investigations of performance and operations in turbomachinery, heat exchangers and other engineering applications. The impact of the molecular complexity on flows with diabatic walls and friction is then evaluated in section 3.

Future work will provide more insights about the influence of the friction coefficient on the entropy loss coefficient in Fanno flows and preliminary results for the mixing of two streams in affected by NICFD effects.

2. THEORETICAL FRAMEWORK FOR NON IDEAL COMPRESSIBLE FLOWS

One-dimensional analyses of steady state compressible flow with mass, momentum, and energy addition under the dense gas assumption can be developed starting from the conservation equations for a control volume of a one-dimensional channel. Variation of cross-section area A, frictional stresses τ_w on the walls, specific shaft work $đw_{\text{shaft}}$, and specific heat addition $đq$ are treated as inputs to the problem. Additional equations are provided by the thermodynamic model of the single-phase fluid in the form $p = Z\rho RT$, where Z is the compressibility factor, and $c_p = c_p(T, p)$. One-dimensional conservation equations allow to derive a new set of differential equations for thermodynamic and fluid dynamic variables such as pressure, density, flow speed and Mach number. Influence coefficients dependent on Mach number and fluid parameters relate each variable to each input variable. Table 1 reports the influence coefficients for one dimensional flows: the variation of each quantity on the first columns is given by the scalar product of the influence coefficients on the corresponding row and the inputs listed on the first row. Table 1 constitutes a generalization of the table devised by Shapiro (1953) to the case of fluid flows affected by NICFD effects. The case of ideal gas flows was later documented also by Greitzer et al. (2004). Cheng et al. (2012) derived a similar table of influence coefficients in terms of different thermodynamic variables, namely an equivalent heat capacity ratio K and a general isentropic index k_s. However, no coefficients for the transfer of shaft work to the fluid were derived. The way quantities are listed in Table 1 is useful because it allows to relate each of the inputs to the variation of all variables through the corresponding influence coefficient, and because it facilitates the study of the effect of each input on the flow separately from all the remaining inputs.

2.1 Fluid properties for NICFD processes

Table 2 lists all the fluid properties involved in the definition of the influence coefficients. According to Baltadjiev et al. (2015), an isentropic NICFD flow can be described by two relations in the form pv^{n_s} = const. and Tp^{-m_s} = const. As reported in reported in Table 2, the Grüneisen parameter G is the product of the isoentropic exponents, n_s and m_s. In solids, this parameter is proportional to the variation of the lattice vibrational spectrum with respect to changes in volume at constant temperature. Arp et al. (1984) extended the definition of G to fluids in the gaseous state through the formulation displayed in Table 2.

Figure 1 shows the variation of the Grüneisen parameter over the temperature-entropy diagram for carbon dioxide (CO_2) and isobutane (i-C_4H_{10}). An in-house code (Colonna et al., 2019) is used to calculate all fluid properties. Lower values of G characterize the isobutane, i.e., the substance with higher molar mass, over the whole Ts diagram.

Table 1: Influence coefficients for compressible channel flow and real gas in terms of γ, Γ, n_s and the Grüneisen parameter G. On the last column, C_f is the friction coefficient and d_H the hydraulic diameter of the channel.

	$\frac{\mathrm{d}A}{A}$	$\frac{\delta q}{c_p T}$	$\frac{\delta w_\mathrm{shaft}}{c_p T}$	$4C_\mathrm{f}\frac{\mathrm{d}x}{d_\mathrm{H}}$
$\frac{\mathrm{d}\rho}{\rho}$	$\frac{M^2}{1-M^2}$	$-\frac{(\gamma-1)}{G}\frac{1}{1-M^2}$	$-\frac{(\gamma-1)}{G^2}\frac{1}{1-M^2}$	$-\frac{G+1}{2}\frac{M^2}{1-M^2}$
$\frac{\mathrm{d}p}{p}$	$\frac{n_s M^2}{(1-M^2)}$	$-\frac{n_s(\gamma-1)M^2}{G(1-M^2)}$	$-\frac{n_s(\gamma-1)}{G^2(1-M^2)}$	$-\frac{n_s M^2}{2}\frac{1+GM^2}{1-M^2}$
$\frac{\mathrm{d}T}{T}$	$\frac{GM^2}{1-M^2}$	$-\frac{\gamma M^2-1}{1-M^2}$	$-\frac{(\gamma-1)}{G(1-M^2)}$	$-\frac{G\left[(\gamma M^2-1)G+(\gamma-1)\right]}{(\gamma-1)(1-M^2)}\frac{M^2}{2}$
$\frac{\mathrm{d}M}{M}$	$-\frac{1+(\Gamma-1)M^2}{1-M^2}$	$\frac{(\gamma-1)}{G}\frac{\Gamma}{(1-M^2)}$	$\frac{(\gamma-1)}{G^2}\frac{\Gamma}{1-M^2}$	$\frac{(G+1)}{2}\frac{\Gamma M^2}{1-M^2}$
$\frac{\mathrm{d}u}{u}$	$-\frac{1}{1-M^2}$	$\frac{(\gamma-1)}{G}\frac{1}{1-M^2}$	$\frac{(\gamma-1)}{(G)^2}\frac{1}{1-M^2}$	$\frac{G+1}{2}\frac{M^2}{1-M^2}$
$\frac{\mathrm{d}a}{a}$	$\frac{(\Gamma-1)M^2}{1-M^2}$	$-\frac{(\Gamma-1)(\gamma-1)}{G}\frac{1}{(1-M^2)}$	$-\frac{(\gamma-1)}{G^2}\frac{\Gamma-1}{1-M^2}$	$-\frac{(G+1)}{2}\frac{(\Gamma-1)M^2}{1-M^2}$
$\frac{\mathrm{d}s}{c_p}$	0	1	0	$\frac{G^2}{\gamma-1}\frac{M^2}{2}$
$\frac{\mathrm{d}h}{c_p T}$	$\frac{G^2}{\gamma-1}\frac{M^2}{1-M^2}$	$-\frac{M^2(G+1)-1}{(1-M^2)}$	$-\frac{1}{1-M^2}$	$-\frac{G^2(G+1)}{(\gamma-1)(1-M^2)}\frac{M^4}{2}$

Table 2: Fluid properties and corresponding definitions.

Property	Symbol	Definition	Ideal gas assumption
Isobaric compressibility	β_p	$\frac{1}{v}\left(\frac{\partial v}{\partial T}\right)_p = \frac{1}{T}+\frac{1}{Z}\left(\frac{\partial Z}{\partial T}\right)_p$	$\frac{1}{T}$
Isothermal compressibility	β_T	$-\frac{1}{v}\left(\frac{\partial v}{\partial p}\right)_T = \frac{1}{p}+\frac{1}{Z}\left(\frac{\partial Z}{\partial p}\right)_T$	$\frac{1}{p}$
Isentropic exponent n°1	n_s	$\frac{\gamma}{\beta_T p}$	γ
Isentropic exponent n°2	m_s	$\frac{\gamma-1}{\gamma}\frac{\beta_T p}{\beta_p T}$	$\frac{\gamma-1}{\gamma}$
Fundamental derivative of gas dynamics	Γ	$1+\frac{\rho}{c}\left(\frac{\partial c}{\partial \rho}\right)_s$	$\frac{\gamma+1}{2}$
Grüneisen parameter	G	$\frac{1}{\rho c_v}\left(\frac{\partial p}{\partial T}\right)_\rho = \frac{\gamma-1}{\beta_P T} = n_s m_s$	$\gamma-1$

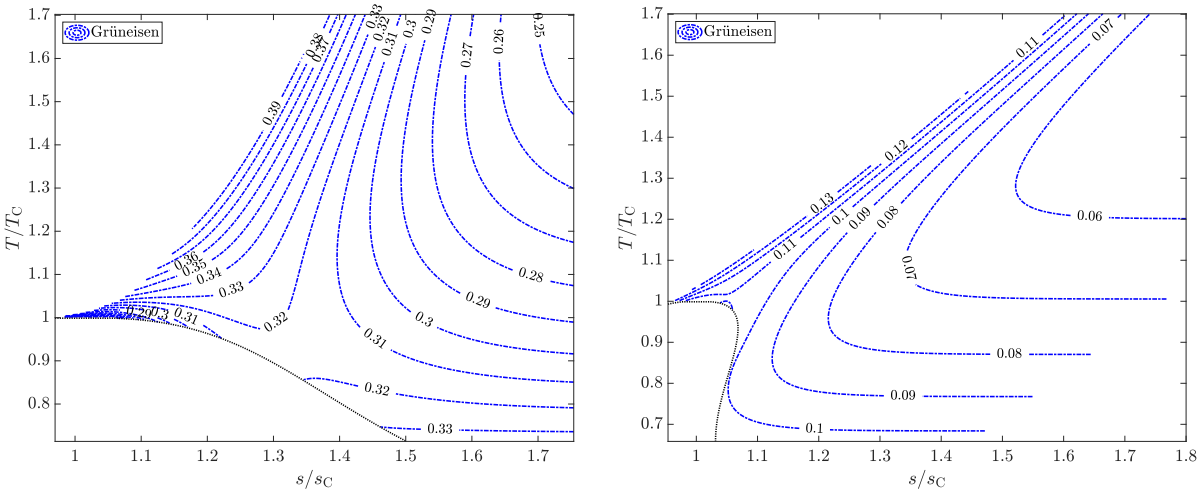

(a) CO_2 **(b) isobutane**

Figure 1: Distribution of the Grüneisen parameter over the *Ts* diagram for fluids with different molecular complexity.

Table 3: Average value of the Grüneisen parameter over an isentropic (s/s_C = 1.4, T/T_C ranging from 0.9 to 1.1) and an isothermal process (T/T_C = 1, s/s_C ranging from 1.25 to 1.45). The deviation is computed with respect to the average value.

	N_2	CO_2	isobutane	MDM
average G isentrope	0,4	0,3	0,071	0,018
max deviation	0, 1%	1, 4%	9%	32%
average G isothermal	0, 4	0, 32	0, 072	0, 018
max deviation	2%	2%	6%	5%

The value of the Grüneisen parameter depends also on the thermodynamic state of the fluid. Table 3 reports the average value of G and its maximum deviation computed over both an isothermal and an isentropic process. In the isentropic case, s/s_C = 1.4 and T/T_C varies from 0.9 to 1.1, with the subscript C denoting the critical quantities; in the isothermal case, T/T_C = 1 and s/s_C varies from 1.25 to 1.45 Fluids with different molecular complexity are evaluated. Deviations from the average value over the considered process are smaller for the isothermal case (< 6% for all fluids). On the other hand, higher molecular complexity implies higher variations of G over an isentropic process. Nevertheless, a decreasing trend of the average G with molecular complexity over a specific process is observed. Trends derived by Arp et al. (1984) and by Arp (1975) for both nitrogen, n-eicosane $C_{20}H_{42}$ and helium for different fluid regimes confirm these observations.

The Grüneisen parameter is thus inversely proportional to the number of atoms in the fluid molecule. As discussed in the following, this parameter allows to analytically describe the energy repartition for one dimensional NICFD flows.

2.2 Partial validation of the NICFD framework: expansion of a dense vapour in a nozzle

Data collected from the expansion of siloxane MDM in the TROVA nozzle of Politecnico di Milano by Spinelli et al. (2018) are utilized to validate the equations applicable to isentropic flows in variable cross-section channels that can be obtained from the combination of the terms in the first column of Table 1. Figure 2a shows the static pressure evolution over the divergent part of the nozzle for p_t/p_C = 0.32 and T_t/T_C = 0.92. Total conditions are denoted by the subscript t. Measurements are compared with the solution provided by the equations for both the NICFD case (Table 1) and the ideal gas case. For the ideal

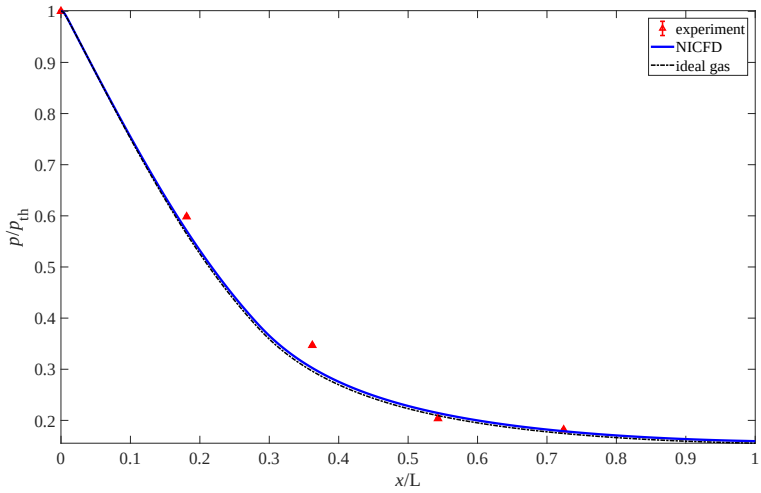

(a)

	T_{in}/T_C	Z_{in}	M_{in}
case 1	1	0.65	0.5
case 2	0.9	0.85	0.8
case 3	1	0.65	0.5
case 4	0.9	0.85	0.8

(b)

Figure 2: (a) Pressure variation over the divergent section of the TROVA nozzle. Experimental results with error bars from Spinelli et al. (2018) are compared with the analytical solution for NICFD (Table 1) and ideal gas flows. The throat is located at $x/L = 0$, with L denoting the length of the divergent section of the nozzle. (b) Inlet conditions for Rayleigh and Fanno flow simulations. T_C denotes the critical temperature.

gas case, the value of γ evaluated at the throat section is kept constant over the nozzle. The calculated pressure matches well the experimental data: the relative difference among them never exceeds 4.5%. The relative error between the NICFD pressure calculated at the outlet section and its value calculated with the ideal gas assumption is low (~ 2.5%) due to the value of the compressibility factor Z in the divergent section being very close to unity.

3. PARADIGMATIC NICFD FLOWS

The second and the fourth column in Table 1 provide the terms that are needed to formulate the equations valid for one-dimensional flows with energy transfer as heat to the fluid and friction over the channel walls. These two effects are analysed separately. The flow with constant heat addition is commonly known as Rayleigh flow, while the flow with wall friction is the Fanno flow, see Anderson (1990). Cramer (2006) and Cramer et al. (1994) provide a qualitative analysis of Rayleigh and Fanno processes in dense vapours using the van der Waals equation of state for fluid property estimations. These simple flow configurations are representative of actual processes in engineering applications. On the one hand, non adiabatic flows can be encountered, for example in small scale turbines for ORC systems and heat exchangers. On the other hand, friction over the blades constitutes one of the loss mechanisms in turbomachinery identified by Denton (1993). The relevant cases of the flow in a duct of a heat exchanger and that of a non-adiabatic turbine can thus be conveniently investigated by means of a simplified model combining the Fanno and the Rayleigh flow.

The numerical solution of the equations valid for the Rayleigh and the Fanno flow, see Table 1, are obtained with a first order forward scheme. Fluids with different levels of molecular complexity are considered: nitrogen (N_2), oxygen (O_2), carbon dioxide (CO_2), methane (CH_4), isobutane, toluene, MM, MDM and D6. For each fluid, four simulations at different inlet conditions are performed (Figure 2b). To ensure thermodynamic and fluid dynamic similarity among all fluids, inlet conditions are prescribed in terms of reduced temperature, compressibility factor and Mach number. For each flow configuration, 40 simulations were therefore performed.

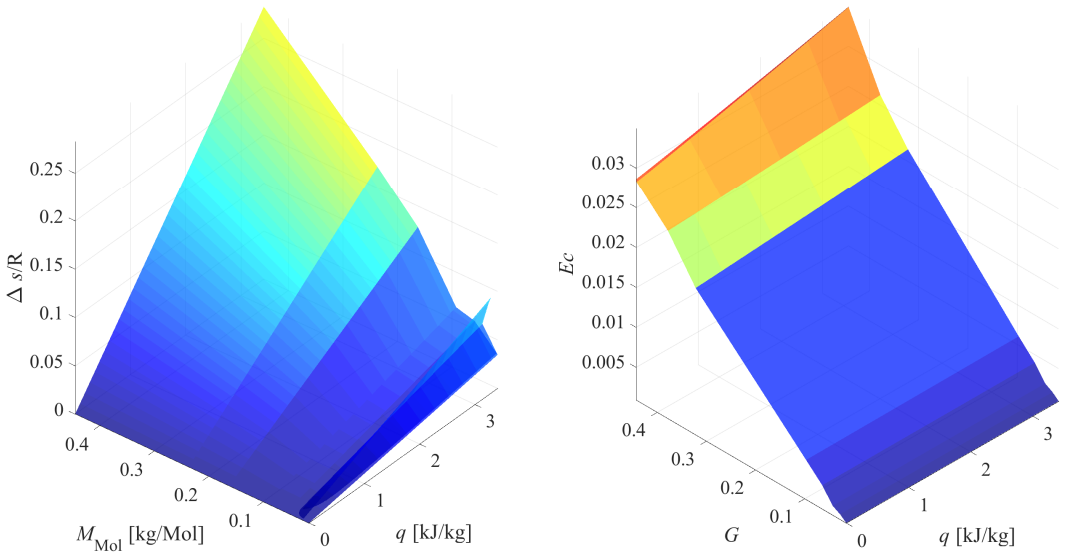

Figure 3: Influence of the fluid properties on Rayleigh processes for case 1 (Figure 2b). (a) entropy increase $\Delta s = s - s_{in}$ with heat. Δs is scaled by the gas constant of the fluid. (b) Eckert number variation with heat in a Rayleigh process.

3.1 Flow with constant energy transfer as heat to the fluid

For all simulations, 3.5 kJ/kg of energy per unit mass is transferred as heat to the fluid. The relation between specific heat and channel length is linear. The derivative $\mathrm{d}q/\mathrm{d}x$ and the length of the infinitesimal control volume $\mathrm{d}x$ are constant all cases reported in Figure 2b. The process is reversible: no losses occur in this flow configuration.

The number of atoms in the fluid molecule influences both the entropy increase in a Rayleigh process and the repartition between specific kinetic and thermal energy. The 3D plot in Figure 3a shows, for case 1, the increase of specific entropy over a Rayleigh process normalized by the gas constant in relation to the energy per unit mass transferred as heat to the system and the molar mass of the fluid. At fixed inlet conditions, the increase of entropy over the process is higher for fluids made of complex organic molecules than for biatomic or triatomic substances. All cases from Figure 2b show similar trends. As a matter of fact, being the entropy increase only due to energy transfer as heat in a Rayleigh flow, the ratio $\Delta s/R$ depends on the molar mass through the relation

$$\frac{\Delta s}{R} \propto \frac{\Delta q}{T}\mathcal{M}, \tag{1}$$

where $\mathcal{M}$ is the molar mass. The molar mass of the molecule thus infuences the specif entropy generation of a Rayleigh process. Influence coefficients of Table 1 allow to derive relations for the variation of specific kinetic energy (K) and specific enthalpy with the heat transferred to the fluid. Knowing from Baltadjiev (2012) that

$$K = \frac{u^2}{2} = \frac{1}{2}\frac{G^2M^2}{(\gamma-1)}c_pT, \tag{2}$$

one can get

$$\frac{\mathrm{d}h}{\mathrm{d}q} = -\frac{(G+1)M^2-1}{1-M^2}, \tag{3}$$

$$\frac{\mathrm{d}K}{\mathrm{d}q} = G\frac{M^2}{1-M^2}. \tag{4}$$

in a Rayleigh process, the Grüneisen parameter is thus the fluid property that influences the repartition of the energy transferred to the fluid molecules among kinetic and thermal energy. Figure 4 shows, for

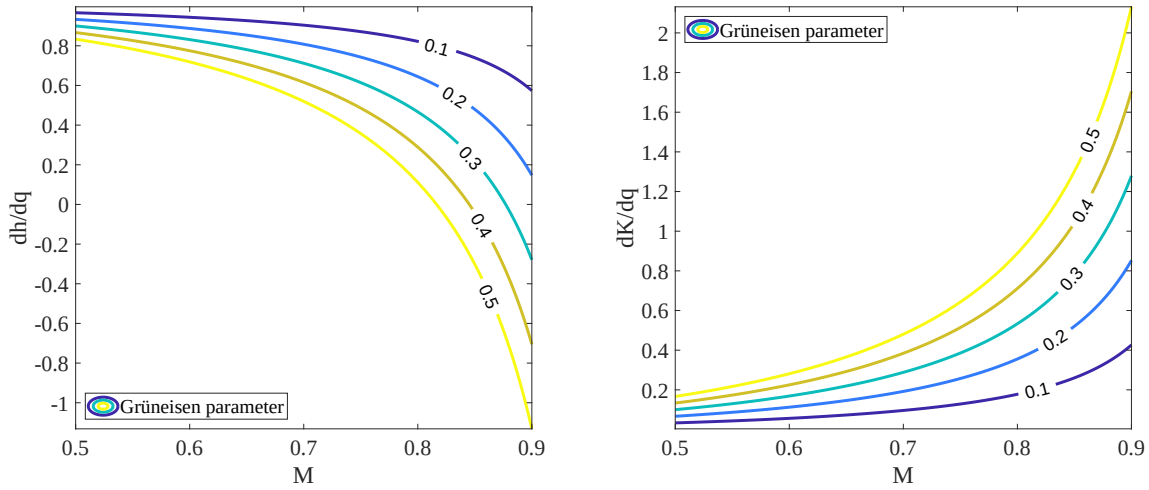

Figure 4: Variation of $\mathrm{d}h/\mathrm{d}q$ and $\mathrm{d}K/\mathrm{d}q$ with Mach number for different values of the Grüneisen parameter.

different values of G, the variation of variables defined by Equation 3 and Equation 4 with the Mach number. The trends show that $\mathrm{d}K/\mathrm{d}q \to 0$ and $\mathrm{d}h/\mathrm{d}q \to 1$ when $G \to 0$. For this limit case, the heat transferred to the fluid increases its specific enthalpy with a linear trend but does not alter its kinetic energy, regardless of the Mach number. Figure 3b shows the variation of the Eckert number, defined as

$$Ec = \frac{u^2}{c_p T} = \frac{G^2}{\gamma - 1} M^2, \tag{5}$$

with the energy per unit mass transferred as heat and with G for case 1. This non dimensional number quantifies the ratio between specific the kinetic energy and the specific thermal energy of the flow. For high G, the Eckert number is high and increases with the energy as heat transferred to the system and, according to Table 1, with the Mach number. The value of the Eckert number decreases with G and tends to 0 for $G \to 0$, regardless of the energy as heat added to the system. Similar trends are observed also for the other cases in Figure 2b. However, for high G values, the higher the inlet Mach number, the higher the Eckert number and its variation with the specific heat, in agreement with Equation 4 and Equation 5.

The Grüneisen parameter fixes also the value of the Mach number at which the flow reaches the maximum specific enthalpy. For Rayleigh processes in NICFD, one can derive, from Equation 3, that

$$M_{\max(h)} = \frac{1}{\sqrt{G+1}}. \tag{6}$$

The lower the Grüneisen parameter, the higher the Mach number required to reach the maximum in specific enthalpy. For siloxanes, $M_{\max(h)} \sim 1$: as a consequence, these flows never reach a maximum in specific enthalpy before choking occurs.

3.2 Flow with wall friction

For the Fanno flow, a straight channel of 0.15 m of lenght and constant hydraulic diameter of $d_H = 0.1$ m is considered. The friction coefficient is set to 0.01 for all fluids. The flow field is numerically solved within each control volume of constant length $\mathrm{d}x$: the Fanno parameter $4C_f\mathrm{d}x/d_H$ is thus constant for all fluids at all conditions.

Entropy generation in Fanno processes can be evaluated in terms of entropy loss coefficient, ζ. From Table 1 and the relation $u^2 = G^2 M^2 c_p T/(\gamma - 1)$, one can derive

$$\zeta = \int_{s_{\text{in}}}^{s_{\text{out}}} \frac{T\mathrm{d}s}{\frac{1}{2}u^2} = \int_0^L \frac{4C_{\text{f}}\mathrm{d}x}{d_{\text{H}}}, \tag{7}$$

where u is the local flow speed. Regardless of fluid properties and Mach number, all fluids thus follow the same trend over the channel length for a given hydraulic diameter. However, the assumption of constant friction coefficient for all fluids is not representative of the actual physics and wrong conclusions can be drawn if its actual variation is not taken into account.

4. CONCLUSIONS

A newly derived theoretical framework based on the definition of a set of influence coefficients relating the change of flow variables to heat addition, wall friction, shaft work and change in cross-section area allows to study one dimensional flows in non ideal compressible fluid dynamics (NICFD). Equations for isentropic flows in variable cross section channels were successfully compared with measurements of the expansion of siloxane MDM in a convergent-divergent nozzle. The Grüneisen parameter emerged as a key quantity for the analysis of NICFD flows. Its average value over isentropic and isothermal processes shows an inverse dependence from molecular complexity. Moreover, it affects the energy repartition within a fluid subjected to Rayleigh processes: the lower G, the lower the increase in kinetic energy with energy transfer as heat and the ratio between specific kinetic and thermal energy. To the authors' opinion, the Grüneisen parameter is a useful quantity to consider also for future investigations on NICFD applications, in particular turbomachinery. The entropy loss coefficient in Fanno processes depends only on the channel width and on the friction coefficient. Further investigations will be performed with regards to the estimation of the friction coefficient of dense vapours in NICFD.

ACKNOWLEDGEMENT

This research has been supported by the Applied and Engineering Sciences Domain (TTW) of the Dutch Organization for Scientific Research (NWO), Technology Program of the Ministry of Economic Affairs, grant number 15837.

REFERENCES

J. D. Anderson. *Modern Compressible Flow: With Historical Perspective*. McGraw-Hill, 2 edition, 1990. ISBN 0-07-001673-9 978-0-07-001673-6.

V. Arp. Thermodynamics of single-phase one-dimensional fluid flow. *Cryogenics*, 15(5):285–289, May 1975. ISSN 00112275. doi: 10.1016/0011-2275(75)90120-4.

V. Arp, J. M. Persichetti, and G.-b. Chen. The Grüneisen Parameter in Fluids. *Journal of Fluids Engineering*, 106(2):193, 1984. ISSN 00982202. doi: 10.1115/1.3243100.

S. Bahamonde, M. Pini, C. De Servi, A. Rubino, and P. Colonna. Method for the Preliminary Fluid Dynamic Design of High-Temperature Mini-Organic Rankine Cycle Turbines. *Journal of Engineering for Gas Turbines and Power*, 139(8):082606, Mar. 2017. ISSN 0742-4795. doi: 10.1115/1.4035841.

N. Baltadjiev. *An Investigation of Real Gas Effects in Supercritical CO2 Compressors*. PhD thesis, Massachussets Institute of Technology, Cambridge, Massachussets, Sept. 2012.

N. D. Baltadjiev, C. Lettieri, and Z. S. Spakovszky. An Investigation of Real Gas Effects in Supercritical CO2 Centrifugal Compressors. *Journal of Turbomachinery*, 137(9):091003, Sept. 2015. ISSN 0889-504X. doi: 10.1115/1.4029616.

D. Cheng, X. Fan, and M. Yang. Quasi-1d Compressible Flow of Hydrocarbon Fuel. In *48th AIAA/ASME/SAE/ASEE Joint Propulsion Conference & Exhibit*, Atlanta, Georgia, July 2012. American Institute of Aeronautics and Astronautics. ISBN 978-1-60086-935-8. doi: 10.2514/6.2012-4090.

P. Colonna, E. Casati, C. Trapp, T. Mathijssen, J. Larjola, T. Turunen-Saaresti, and A. Uusitalo. Organic Rankine Cycle Power Systems: From the Concept to Current Technology, Applications, and an Outlook to the Future. *Journal of Engineering for Gas Turbines and Power*, 137(10):100801, Oct. 2015. ISSN 0742-4795. doi: 10.1115/1.4029884.

P. Colonna, T. P. van der Stelt, and A. Guardone. FluidProp (Version 3.1): A program for the estimation of thermophysical properties of fluids, 2019. URL `http://www.asimptote.nl/software/fluidprop`. A computer program since 2004.

M. S. Cramer. Rayleigh processes in single-phase fluids. *Physics of Fluids*, 18(1):016101, Jan. 2006. ISSN 1070-6631, 1089-7666. doi: 10.1063/1.2166627.

M. S. Cramer, J. F. Monaco, and B. M. Fabeny. Fanno processes in dense gases. *Physics of Fluids*, 6(2): 674–683, Feb. 1994. ISSN 1070-6631, 1089-7666. doi: 10.1063/1.868307.

C. De Servi, M. Burigana, M. Pini, and P. Colonna. Design method and performance prediction for radial-inflow turbines of high-temperature mini-Organic Rankine Cycle power systems. *Accepted manuscript for ASME*, 2019.

J. D. Denton. Loss Mechanisms in Turbomachines. In *Volume 2: Combustion and Fuels; Oil and Gas Applications; Cycle Innovations; Heat Transfer; Electric Power; Industrial and Cogeneration; Ceramics; Structures and Dynamics; Controls, Diagnostics and Instrumentation; IGTI Scholar Award*, page V002T14A001, Cincinnati, Ohio, USA, May 1993. ASME. ISBN 978-0-7918-7889-7. doi: 10.1115/93-GT-435.

E. M. Greitzer, C. S. Tan, and M. B. Graf. *Internal Flow: Concepts and Applications*. Cambridge University Press, Cambridge, 2004. ISBN 978-0-511-61670-9. doi: 10.1017/CBO9780511616709.

A. Kluwick. Non-Ideal Compressible Fluid Dynamics: A Challenge for Theory. *Journal of Physics: Conference Series*, 821:012001, Mar. 2017. ISSN 1742-6588, 1742-6596. doi: 10.1088/1742-6596/821/1/012001.

K. Rosset, V. Mounier, E. Guenat, and J. Schiffmann. Multi-objective optimization of turbo-ORC systems for waste heat recovery on passenger car engines. *Energy*, 159:751–765, Sept. 2018. ISSN 03605442. doi: 10.1016/j.energy.2018.06.193.

A. H. Shapiro. *The Dynamics and Thermodynamics of Compressible Fluid Flow*, volume 1. The Ronald Press Company, New York, NY (now John Wiley & Sons, New York, NY), 1953.

A. Spinelli, G. Cammi, S. Gallarini, M. Zocca, F. Cozzi, P. Gaetani, V. Dossena, and A. Guardone. Experimental evidence of non-ideal compressible effects in expanding flow of a high molecular complexity vapor. *Experiments in Fluids*, 59:126, 2018. doi: 10.1007/s00348-018-2578-0.

P. A. Thompson. A Fundamental Derivative in Gasdynamics. *Physics of Fluids*, 14(9):1843, 1971. ISSN 00319171. doi: 10.1063/1.1693693.